The International Archives of the Photogrammetry, Remote Sensing and Spatial Information Sciences, Volume XLVIII-M-9-2025
30th CIPA Symposium “Heritage Conservation from Bits:
From Digital Documentation to Data-driven Heritage Conservation”, 25–29 August 2025, Seoul, Republic of Korea

Research on the Hyperspectral-based Unmixing Model of Composite Pigments on Mural Surfaces

Yihan Zhang [1,2], Shuqiang Lyu [1,2], Miaole Hou [1,2,*], Jing Guo [3], Junlin Yan [1,2]
1 School of Geomatics and Urban Spatial Informatics, Beijing University of Civil Engineering and Architecture, No.15 Yongyuan Road, Daxing Distict, Beijing, China - 201904010211@stu.bucea.edu.cn, lvshuqiang@bucea.edu.cn, houmiaole@bucea.edu.cn; 2108570424056@stu.bucea.edu.cn.
2 Beijing Key Laboratory for Architectural Heritage Fine Reconstruction & Health Monitoring, No. 15 Yongyuan Road, Daxing District. Beijing. China
3 Yungang Academy, Shanxi 037007, China - 541958911@qq.com.

Keywords: Hyperspectral, Pigments, Unmixing model, Mural, Linear model.

Abstract

Murals constitute an invaluable component of cultural heritage, encapsulating profound artistic and historical significance. Hyperspectral remote sensing, as a non-destructive testing technique, offers an effective means for analysing and identifying mural pigments. We proposed a spectral unmixing method based on the negative logarithm of spectral reflectance, aimed at improving the accuracy of quantitative analysis for composite pigments in murals. We obtained three sets of mixed spectra: cinnabar-orpiment, azurite-orpiment, and azurite-malachite. The original reflectance was converted into negative logarithmic values, and linear models were applied for unmixing. Supervised unmixing was conducted in the experiment to evaluate the model’s precision, with the unmixing process carried out using known endmembers. The unmixing accuracy was quantified using the Root Mean Square Error, which compares the estimated abundances of all endmembers with actual values. Additionally, a comparison was made between the negative logarithmic transformation and the commonly used transformations of original reflectance, first derivative, and second derivative. The result show that the logarithmic hyperspace linear model simplifies spectral unmixing complexity, enhancing the accuracy of linear unmixing models in addressing mixed pigment unmixing problems. To validate the effectiveness of the proposed method for real murals, the improved model was applied to the hyperspectral data unmixing analysis of murals collected by the Yungang Academy, located in Shanxi Province, China. Experimental findings demonstrate that, compared to traditional methods, the improved unmixing approach more precisely represents the pigment distribution in the murals. This study offers new ideas and methods for the digital preservation and restoration of mural composite pigments.

1. Introduction

Ancient murals are invaluable cultural relics that reflect the social life and culture of their time, possessing significant artistic value. The pigment layers of these murals not only contain rich historical and cultural information but also serve as key evidence for studying ancient artistic techniques and social development. However, due to environmental erosion and natural aging, mural pigments commonly suffer from degradation phenomena such as fading and peeling. This makes the need for precise analysis and scientific preservation using modern technological methods particularly urgent. In recent years, pigment identification and unmixing techniques for murals have become a research hotspot in the field of cultural heritage conservation. Extensive research employed micro-Raman spectroscopy and SEM-EDS analysis to identify an unusual yellow pigment in the Tang Dynasty tomb murals (Liu, 2023). Extensive study employed multi-analytical characterization to identify synthetic ultramarine and emerald green pigments in Ming Dynasty North Mosque murals (Dong, 2023). The 1795 Athonite murals in Bulgaria's Rila Monastery using OM, ATR-FTIR, SEM-EDS, and ELISA, identifying traditional pigments with egg tempera binders, except for carbohydrate-bound smalt in blue backgrounds, establishing this work as a technical reference for later Balkan iconography (Stamboliyska, 2024). characterized Rafael Coronel's 20th century mural Paisaje Abstracto using OM, SEM-EDS, NMR, ATR-FTIR and GC/MS, identifying an unconventional poly methyl methacrylate painting medium containing cadmium sulfide and titanium dioxide pigments, along with polymerization additives, revealing the technical origins of its severe aging-induced fractures (Aguilar-Rodríguez, 2023). The study of mural pigments is currently a major research hotspot. To enrich the colors of murals, ancient painters often mixed multiple pigments to create new colors. Determining the proportion of pure pigments in the mixed pigments is crucial for better mural restoration, making pigment unmixing essential. Hyperspectral technology, with its non-invasive, rapid, and efficient advantages, enables comprehensive analysis of large mural areas, making it an ideal choice for cultural heritage conservation.

A single pixel in the hyperspectral image may be described as a mixture of the spectruma of the pure pigments present in this pixel. The pure pigment spectra are regarded as endmember spectra and the proportion of the pure pigment is regarded as its abundance. The unmixing process is based upon mixing models that describe the physical processes that occur when different pigments are mixed. They can be classified as linear or non-linear. In linear models, the mixed spectrum is obtained from a linear combination of endmember weighted by the concentrations. It is commonly used in remote sensing and is assumed as an acceptable approximation in many real scenarios (Stagakis, 2016). Its assets are physical interpretability, computational tractability, and ease of implementation (Zhang, 2022). It has been used in the field of cultural heritage with promising results. For instance, Some rearch employed fully constrained least squares (FCLS) for the pigment mapping of The Scream (1893) painting, under the assumption that the endmembers were known(Deborah, 2014). This approach can recognize the mixture of some percentage of different pigments. The experiment used azurite and malachite as examples to perform spectral unmixing of mixed spectra using the FCLS method, exploring the spectral mixing model of these two mineral pigments (Zhao, 2018). We found that by applying mathematical transformations to the original reflectance, the

spectral linear characteristics can be enhanced. performed high-precision non-destructive detection of mural salts by applying the reciprocal logarithmic transformation to the original reflectance data combined with the random forest model (Guo, 2023). The research established a hyperspectral conductivity feature inversion model for murals by integrating fractional-order derivative transformation of the original reflectance with the least squares model, providing an effective technical method for monitoring murals and other precious cultural heritage (Ren, 2024). Therefore, this paper will focus on the practical application of composite pigment unmixing by applying a negative logarithmic transformation to the original spectral reflectance combined with a linear unmixing model.

This paper employs laboratory experiments to investigate methods for determining mixed pigment proportions on mural surfaces, with the aim of providing a non-destructive and more efficient analytical approach for mixed pigments, thereby establishing a more scientific basis for mural pigment restoration. Mixed pigment samples were prepared in the laboratory and corresponding spectral data were collected. The original reflectance was processed using first-order derivative (FOD), second-order derivative (SOD), and negative logarithmic (NL) transformation, combined with the FCLS model for unmixing. Model accuracy was evaluated using Root Mean Square Error (RMSE), and the highest-accuracy model was applied to a mural, created in Qing Dynasty (1636-1912 AD) to evaluate its unmixing performance.

2. Materials and Acquisitions

2.1 Materials Preparation

Through repeated practice over extended periods, pigment usage had gradually developed established conventions and painting techniques. After meticulous investigation and comparison, we selected azurite, malachite, cinnabar, and orpiment as study objects, which are the most commonly used mineral pigments in traditional Chinese paintings, as shown in Figure 1. They represent the quintessential pigments for blue, green, red, and yellow hues, respectively (Lyu, 2021). Three groups of mixed pigment samples were prepared by combining cinnabar and orpiment, azurite and orpiment, as well as azurite and malachite in seven distinct mass ratios in Figure 2. In order to guarantee the quality of the pigments, samples for the blending study were prepared using powdered minerals sourced from JiangSixutang, a prestigious traditional pigment manufacturer with a history spanning three centuries. As mineral pigment powder cannot be directly applied to substrates, traditional painting employs various binder materials including animal proteins, polysaccharides, or lipids (Zhang, 2019). In this experiment, gelatin produced by JiangSixutang was used as the binder, which closely resembles traditional animal protein-based binders used historically.

Azurite Malachite

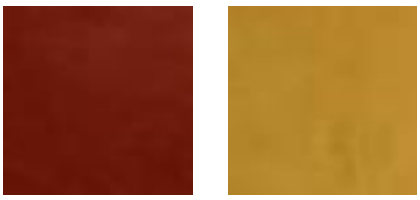

Cinnabar Orpiment

Figure 1. Four pure pigment samples.

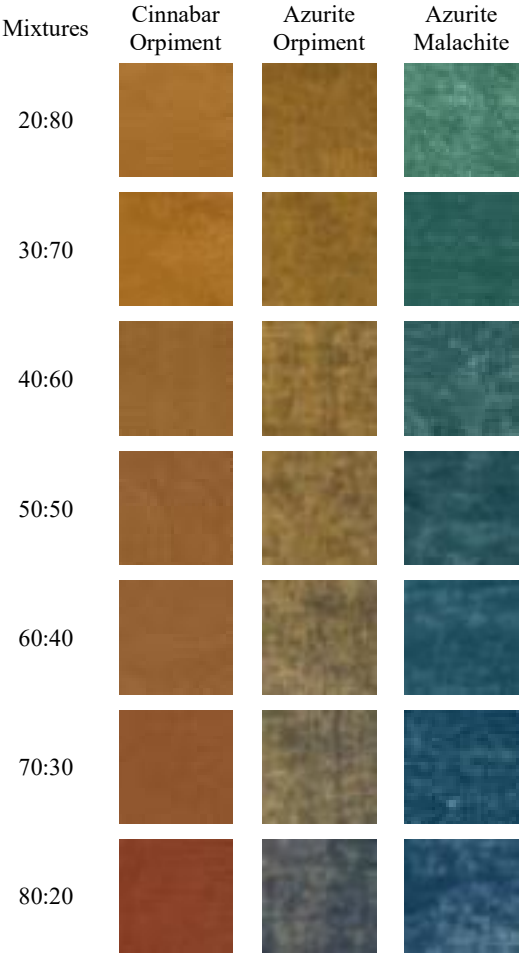

Figure 2. Mixed pigments samples.

2.2 Data Acquisition

In this study,the reflectance spectra of the samples were collected using an ASD-FieldSpec4HI-RES spectrometer. The specific parameters of this instrument are shown in Table 1. The data collection was carried out in a darkroom, with a halogen lamp as the only light source.

Name	Parameters
Spectral range	350-2500nm
Spectral width	2.5nm
Spectral resolution	3nm @ 700nm 8nm @ 1400/2100 nm
Number of bands	2151
Size	12.7x35.6x29.2 cm
Weight	5.44 kg

Table 1. Specifications of ASD-Field Spec 4 portable spectroradiometer.

The instrument used to capture the hyperspectral image of the mural sample was a Themis Vision Systems VNIR400H .The data collection also was carried out in a darkroom, with a halogen lamp as the only light source. The main specifications of this instrument are shown in Table 2.

Name	Parameters
Spectral	400-1000nm
Number of bands	1040
Spectral width	0.6nm
Spectral resolution	2.6nm
Weight	1.85kg

Table 2. Specifications of hyperspectral imaging spectroradiometer parameters.

The original hyperspectral data are always influenced by the change in environmental parameters and dark current noises. Therefore, it is necessary to using Equation (1):

$$R = \frac{R_{raw} - R_{dark}}{R_{white} - R_{dark}} \times 99\% \quad (1)$$

Where R is the calibrated data, R_{raw} is the collected original hyperspectral data, R_{white} is the standard white board data, and R_{dark} is the dark current noise data.

3. Methods

The overall process of the research on the hyperspectral-based unmixing model of composite pigments on mural surfaces is shown in the Figure 3.The entire process includes sample preparation, data acquisition, data preprocessing, spectral transformation, the unmixing process using the proposed method, accuracy evaluation, and finally, experimental validation using Qing Dynasty murals.

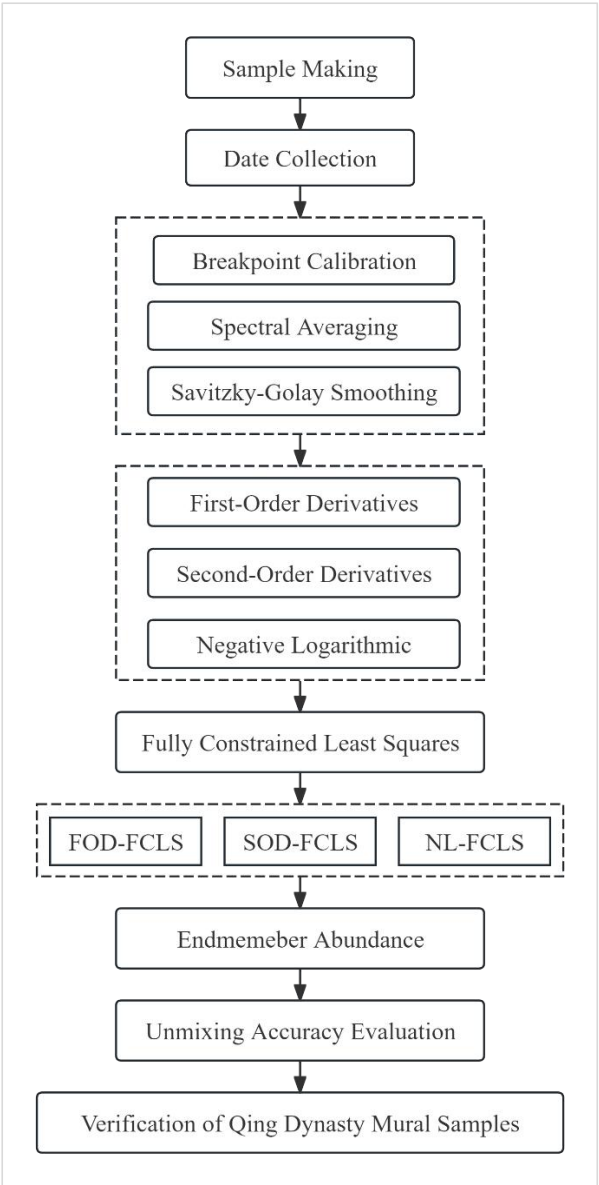

Figure 3. The overall process of the study.

3.1 Fully Constrained Least Squares Unmixing

The linear mixture model (LMM) is a relatively simple and representative model that does not account for the effects of multiple radiation scattering between different surface materials. While this simplicity makes the model easier to understand and apply, it also restricts its applicability in complex surface conditions.

In the linear mixture model, the reflectance of a mixed pixel at a specific wavelength is a linear combination of the reflectance of its endmember components. The LMM formula is expressed in Equation (2):

$$y = \sum_{i=1}^{n} \rho_i a_i + \varepsilon_i = \rho a + \varepsilon = \hat{y} + \varepsilon \quad (2)$$

The linear mixture model combined with the FCLS method can estimate the abundance of each endmember. The endmember abundances can be solved using the following optimization equations, as shown in Equations (3) and (4).

$$\varepsilon = \arg\min \left\| y - \hat{y} \right\|_2 \quad (3)$$

$$s.t. a_i \geq 0, \sum_{i=1}^{n} a_i = 1 \quad (4)$$

In the equations, $y \in R^{m\times 1}$ denotes the measured spectral vector of the mixed pigment, $\hat{y} \in R^{m\times 1}$ represents the estimated mixed spectral vector based on the mixing model. m represents the number of bands, n represents the number of endmembers, ρ is the reflectance of the endmembers, a is the abundance vector of the endmembers, ε is the error term. To reflect real conditions, the abundance vector a typically adheres to two constraints in unmixing algorithms: the non-negativity constraint $a_i \geq 0$ and the sum-to-one constraint $\sum_{i=1}^{n} a_i = 1$.

3.2 Log-Reflectance Hyperspace Linear Unmixing Algorithm

The logarithmic hyperspace linear model simplifies spectral unmixing complexity, enhancing linear unmixing models accuracy in addressing mixed pigment unmixing problems. (Grillini, 2021) explored various mixing models, testing additive and subtractive models of linear image processing, and found that the subtractive model outperformed other models. (Valero, 2023) proposed the simplest method to transform the subtractive model into an additive model by taking the negative logarithm of spectral reflectance data, improving the FCLS method based on this approach.

In the mixing model, the mixed reflectance ρ is a combination of the reflectance ρ_i of the individual endmembers. For the subtractive mixing model, the mixed reflectance is calculated as the product of the reflectance of the individual endmembers, as shown in Equation (5):

$$\rho = \prod_{i=1}^{N} \rho_i^{a_i} \quad (5)$$

ρ_i represents the reflectance of the i endmember, a_i is the abundance weight of the endmember and $\sum_{i=1}^{n} a_i = 1$. Transforming it into logarithmic space involves taking the negative logarithm of the mixed reflectance ρ, as shown in Equation (6):

$$-\log(\rho) = -\log(\prod_{i=1}^{N} \rho_i^{a_i}) \quad (6)$$

According to the properties of logarithms, the logarithm of a product equals the sum of the logarithms. Through this transformation, the original multiplicative form becomes a linear additive form, as shown in Equation (7), allowing the mixing model in logarithmic space to be treated as a linear model:

$$\rho = \sum_{i=1}^{N} \rho_i a_i \quad (7)$$

-log(ρ) is the mixed reflectance in logarithmic space, *-log(ρᵢ)* is the reflectance of i endmember in logarithmic space. Applying the negative logarithm to the spectral reflectance data transforms the subtractive mixing model into an additive model, thereby enhancing the linear characteristics of the spectral curve. The linear mixing model employed in logarithmic space simplifies spectral unmixing, reduces computational complexity, and improves the unmixing accuracy of the linear model.

3.3 Accuracy Evaluation

The endmembers utilized in this study include azurite, malachite, cinnabar, and orpiment. These pigments were selected due to their frequent use in ancient murals and distinct spectral characteristics. These endmembers were selected based on their representativeness in spectral unmixing, ensuring a comprehensive analysis of different spectral line shapes. The unmixing accuracy is quantified using the Root Mean Square Error (RMSE), which compares the estimated abundances of all endmembers with their actual values. The RMSE is expressed in Equation (8):

$$RMSE = \sqrt{\frac{1}{N}\sum_{i=1}^{N}(a_i - \hat{a}_i)^2} \quad (8)$$

N is the number of combinations in pigment mixtures made from the same pigments, a_i is the actual abundance of the endmembers in the i mixture, $\hat{a}_i$ is the endmember abundance of the i mixture obtained through the unmixing algorithm, The smaller the RMSE, the smaller the error in the abundance inversion and the higher the unmixing accuracy.

4. Result and Analysis

4.1 Unmixing Results

We applied FOD, SOD, and NL transformations to the three sets of mixed pigment spectral data collected, as shown in Figure 4-6. Subsequently, FCLS unmixing was performed, and the results are shown in Table 3-5.

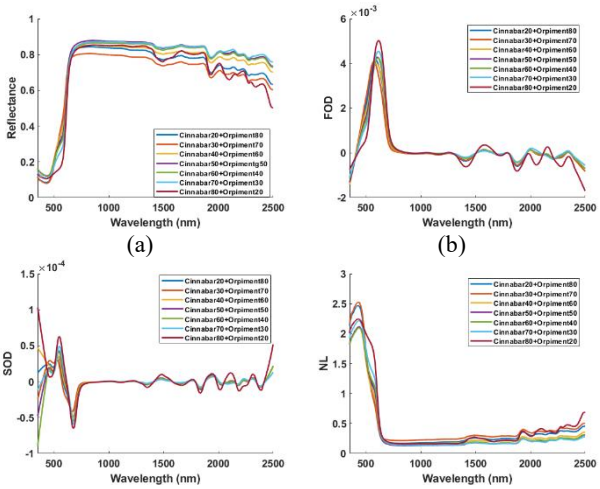

Figure 4. Cinnabar and Orpiment Spectral Transformation: (a) original mixed pigment spectral curves; (b) FOD transformation; (c) SOD transformation; (d) NL transformation.

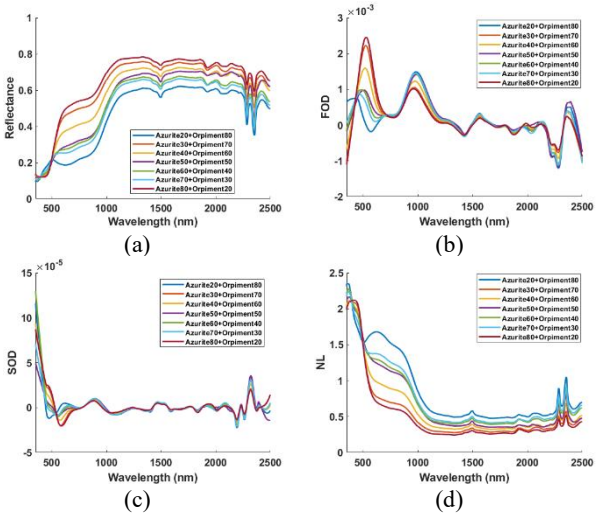

Figure 5. Azurite and Orpiment Spectral Transformation：(a) original mixed pigment spectral curves; (b) FOD transformation；(c) SOD transformation；(d) NL transformation.

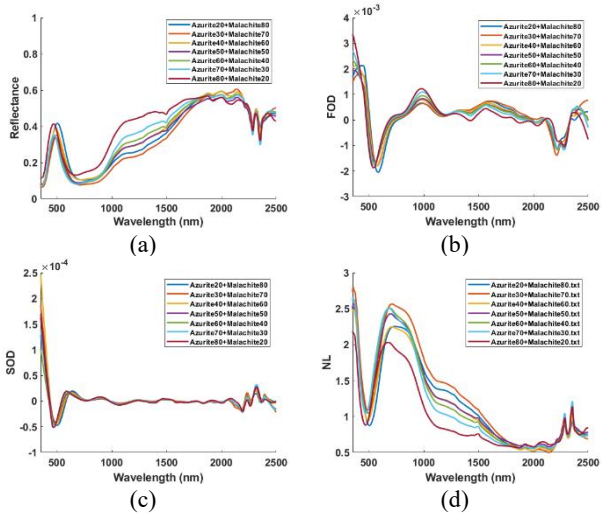

Figure 6. Azurite and Malachite Spectral Transformation：(a) original mixed pigment spectral curves; (b) FOD transformation；(c) SOD transformation；(d) NL transformation

Abundance Measured		0.2	0.3	0.4	0.5	0.6	0.7	0.8	RMSE
	Cinnabar	0.8	0.7	0.6	0.5	0.4	0.3	0.2	
FCLS	Cinnabar	0.1306	0.1841	0.0171	0.0000	0.0535	0.0923	0.4827	0.4112
	Orpiment	0.8694	0.8159	0.9829	1.0000	0.9465	0.9077	0.5173	
FOD-FCLS	Cinnabar	0.4220	0.2949	0.4819	0.5797	0.6261	0.7000	0.8608	0.0976
	Orpiment	0.5780	0.7051	0.5181	0.4203	0.3739	0.3000	0.1392	
SOD-FCLS	Cinnabar	0.2610	0.4905	0.6728	1.0000	0.9999	1.0000	0.7192	0.2978
	Orpiment	0.7390	0.5095	0.3272	0.0000	0.0001	0.0000	0.2808	
NL-FCLS	Cinnabar	0.1269	0.1151	0.0625	0.0972	0.8692	0.7886	0.5711	0.2531
	Orpiment	0.8730	0.8849	0.9373	0.9026	0.1306	0.2112	0.4287	

Table 3. Unmixing Accuracy for the Cinnabar and Orpiment.

Abundance Measured		0.2	0.3	0.4	0.5	0.6	0.7	0.8	RMSE
	Azurite	0.8	0.7	0.6	0.5	0.4	0.3	0.2	
FCLS	Azurite	0.0708	0.1556	0.2550	0.3838	0.4262	0.5459	0.6491	0.1458
	Orpiment	0.9292	0.8444	0.7450	0.6162	0.5738	0.4541	0.3509	
FOD-FCLS	Azurite	0.2295	0.5901	0.4840	0.3723	0.3600	0.3226	0.6314	0.2194
	Orpiment	0.7705	0.4099	0.5160	0.6277	0.6400	0.6774	0.3686	
SOD-FCLS	Azurite	0.4596	0.2202	0.3062	0.4319	0.3766	0.4320	0.8044	0.1832
	Orpiment	0.5403	0.7798	0.6938	0.5681	0.6234	0.5680	0. 1956	
NL-FCLS	Azurite	0.5391	0.1724	0.2569	0.3561	0.6165	0.5809	0.8651	0.1369
	Orpiment	0.4608	0.8274	0.7429	0.6438	0.3835	0.4149	0.1347	

Table 4. Unmixing Accuracy for the Azurite and Orpiment.

Abundance Measured		0.2	0.3	0.4	0.5	0.6	0.7	0.8	RMSE
	Azurite	0.8	0.7	0.6	0.5	0.4	0.3	0.2	
FCLS	Azurite	0.3777	0.3199	0.5191	0.5455	0.6294	0.7554	0.9815	0.1103
	Malachite	0.6223	0.6801	0.4809	0.4545	0.3706	0.2446	0.0185	
FOD-FCLS	Azurite	0.3881	0.4025	0.5296	0.6160	0.6691	0.7589	0.8733	0.1132
	Malachite	0.6119	0.5975	0.4704	0.3840	0.3309	0.2411	0.1267	
SOD-FCLS	Azurite	0.2600	0.2815	0.3022	0.3560	0.4697	0.4505	0.4422	0.1857
	Malachite	0.7400	0.7185	0.6977	0.6439	0.5303	0.5495	0.5578	
NL-FCLS	Azurite	0.3505	0.3621	0.4587	0.5005	0.6218	0.7126	0.8023	0.0650
	Malachite	0.6495	0.6377	0.5413	0.4995	0.3778	0.2870	0.1996	

Table 5. Unmixing Accuracy for the Azurite and Malachite.

From the abundance inversion results in Table 3-5, we can observe that the four algorithms performed differently on the different mixed pigments. The first-order derivative, second-order derivative, and negative logarithmic transformations of the original reflectance have different effects on the unmixing results. For the mixtures of Azurite and Orpiment, as well as

Azurite and Malachite, we found that the RMSE value was smallest and the unmixing accuracy was highest after the negative logarithmic transformation. Moreover, at certain specific mixing ratios, excellent unmixing results were obtained. Additionally, we observed that the unmixing accuracy for these two pigment mixtures was worse after applying derivative transformations compared to using the original reflectance. Interestingly, for the mixture of Cinnabar and Orpiment, the RMSE value was lowest and the unmixing accuracy was highest after applying the first-order derivative transformation, with excellent unmixing results for most ratios, and even complete unmixing accuracy at the 0.7:0.3 ratio. Furthermore, the RMSE for the NL-FCLS model was nearly half of that for the FCLS model, demonstrating good unmixing performance. Based on the three experiments, we conclude that the NL-FCLS model can be considered the preferred model for pigment unmixing, and the first-order derivative transformation is an effective method to improve unmixing accuracy, depending on the specific case.

4.2 Qing Dynasty Murals Application Result

We chose the hyperspectral image collected in Yungang Academy, Datong City, Shanxi Province, China as the verification data for real artefacts, as shown in Figure 7. We used the NL-FCLS model, which has been validated for its effectiveness in practical applications, to unmix the pigments of the mural paintings. The abundance map of pigment unmixing is shown in Figure 8. The experimental results demonstrate that the NL-FCLS model models accurately reflect the abundance distribution of pigments in cultural heritage relics.

Figure 7. Qing dynasty murals.

(a) Endmember 1

(b) Endmember 2

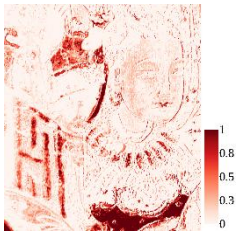

(c) Endmember 3

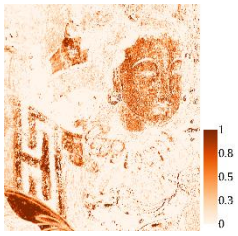

(d) Endmember 4

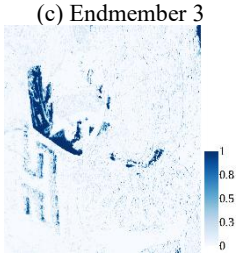

(e) Endmember 5

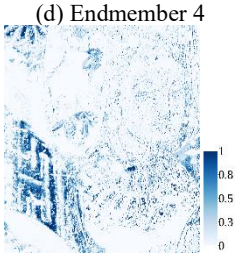

(f) Endmember 6

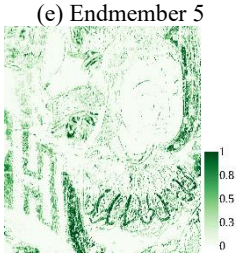

(g) Endmember 7

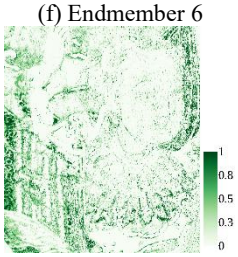

(h) Endmember 8

Figure 8. Abundance maps of NL-FCLS.

5. Conclusions

In this study, we performed various mathematical transformations on the original reflectance data and combined them with the FCLS method for unmixing analysis. It was found that the negative logarithmic transformation effectively enhanced the linear characteristics of the original spectra. We believe that the mixing effects of different components in the original spectral curves may introduce non-linear relationships, and the negative logarithmic transformation significantly improves this non-linearity, making the data better aligned with the linear model assumption. Notably, for the mixed pigment systems of Azurite and Malachite, as well as Azurite and Orpiment, the accuracy of the FCLS linear unmixing model was significantly improved after applying the negative logarithmic transformation. Moreover, in the analysis of Cinnabar and Orpiment mixed pigments, the first-order derivative transformation led to a breakthrough improvement in unmixing accuracy. Through in-depth analysis of the spectral features, we found that the first-order derivative transformation significantly enhanced the spectral sensitivity to wavelength variations, particularly in regions with notable spectral gradient changes. This enhancement allowed the FCLS method to more accurately identify and separate the characteristic signals of different components, greatly improving unmixing performance. To validate the practicality of the method, we successfully applied the Nonlinear Transformation combined with FCLS (NL-FCLS) model to pigment analysis of Qing Dynasty murals in the Yungang Academy, Shanxi, and achieved satisfactory results.

In the future, we will further explore the non-linear mixing mechanisms of mixed pigments and seek more suitable algorithms for pigment unmixing by combining the spectral profile characteristics of different mixed pigments.

References

Liu, Z. J., Xu, W. Z., Zhang, Y. J., Wang, Y. Y., Li, J. W., 2023: Identification of the Pigments on the Mural Paintings from an Ancient Chinese Tomb of Tang Dynasty Using Micro-Raman and Scanning Electron Microscopy/ Energy Dispersive X-ray Spectroscopy Analysis. *Minerals* 13, 1224. doi.org/10.3390/ min13091224.

Dong, S.S., Xiang, J.K., Ji, J., Wang, Y.J., Zhang, G., Fu, P., Han, JW., LI, L., 2023: Multi-Method Analysis of Painting Materials in Murals of the North Mosque (Linqing, China). *Coatings*. 13,1298. doi.org/10.3390/ coatings13071298.

Stamboliyska, B., Tapanov, S., Velcheva, E., Atanasova-Vladimirova, S., Ranguelov, B., Guncheva, M., Stoyanov, S., Yancheva, D., 2024: Materials and Techniques of the Mural Paintings in the Church-Ossuary of the Rila Monastery, Bulgaria. *Minerals.* 14,1115. doi.org/ 10.3390/min14111115.

Aguilar-Rodríguez, P., Zetina, S., Mejía-González, A., Esturau-Escofet, N., 2023: Microanalytical Characterization of an Innovative Modern Mural Painting Technique by SEM-EDS, NMR and Micro-ATR-FTIR among Others. *Molecules*. 28,564. doi.org/10.3390/molecules28020564.

Stagakis, S., Vanikiotis, T., Sykioti, O., 2016: Estimating forest species abundance through linear unmixing of CHRIS/PROBA imagery. *ISPRS J Photogramm Remote Sens*. 119,79–89. doi.org/10.1016/j.isprsjprs.2016.05.013.

Zhang, G., Mei, SH., Xie, BB., Ma, MY., Zhang, YF., Feng, Y., Du, Q., 2022: Spectral variability augmented sparse unmixing of hyperspectral images. *IEEE Trans Geosci Remote Sens.* 60,1–13. doi.org/ 10.1109/TGRS.2022.3169228.

Deborah, H., George, S., Hardeberg, J.Y. (2014). Pigment Mapping of the Scream (1893) Based on Hyperspectral Imaging. In: Elmoataz, A., Lezoray, O., Nouboud, F., Mammass, D. (eds) *Image and Signal Processing*. ICISP 2014: Lecture Notes in Computer Science, vol 8509. Springer, Cham. doi.org/10.1007/978-3-319-07998-1_28.

Li, D.P., Zhao, H.Q., Zhang, L.F., Zhao, X.S., 2018: Preliminary Study in Spectral Mixing Model of Mineral Pigments on Chinese Ancient Paintings-Take Azurite and Malachite for Example. *Spectrosc Spect Anal*.38(8), 2612-2616. doi.org /10.3964/j.issn.1000-0593(2018)08-2612-05.

Guo, Z.Q., Lyu, S.Q., Hou, M.L., 2023: Estimation of the soluble salt concentration in murals based on spectral transformation and feature extraction modelling. *J Appl Spectrosc*. 90,1123–32. doi.org/10.1007/s10812-023-01642-3.

Ren, Y.K., Liu, F., 2024: The spectral inversion model for electrical conductivity in mural plaster following phosphate erosion based on fractional order differentiation and novel spectral indices. *Herit Sci.* 12,286. doi.org/10.1186/s40494-024-01385-0.

Lyu, S.Q., Meng, D., Hou, M.L., Tian, S., Huang, C.H., Mao, J.C., 2021: Nonlinear mixing characteristics of reflectance spectra of typical mineral pigments. *minerals.*11(6),626. doi.org/10.3390/min11060626.

Zhang, S.X., Fang, X.Y., Fu, Q.L., M, Y., Zhang, W.X.,2019. Preliminary study of the pigments on an acrobat figurine excavated from Emperor Qinshihuang’s Mausoleum. Sci Conserv Archaeol. 31(3), 115-121.doi.org/10.16334/j.cnki.cn31-1652/k.2019.03.015

Grillini, F., Thomas, J.B., George, S.,2021. Comparison of Imaging Models for Spectral Unmixing in Oil Painting +. sensors. 21,2471. doi.org/10.3390/s21072471

Valero, E.M., Martínez-Domingo, M.A., López-Baldomero, A.B., López-Montes, A., Abad-Muñoz, D., Vílchez-Quero, J.L., 2023. Unmixing and pigment identification using visible and short-wavelength infrared: Reflectance vs logarithm reflectance hyperspaces. J Cult Herit. 64,290–300.hdoi.org/10.1016/j.culher.2023.10.016